PCCP

Accepted Manuscript

ROYAL SOCIETY OF CHEMISTRY

www.rsc.org/pccp

Size and shape effect on bond number of quantum dots and its relation with thermodynamic properties

H. Li[1*], H.J. Xiao[1], T.S. Zhu[2], H.C. Xuan[1], M. Li[2*]

[1] College of Materials Science and Engineering, Taiyuan University of Technology, Taiyuan 030024, China

[2] School of Physics and Electric Information, Huaibei Normal University, Huaibei, 235000, China

Abstract

Through introducing size (N_t) and shape factor (λ), the size- and shape-dependent bond number B_a of quantum dots respectively with icosahedral, truc-decohedral, cuboctahedral, octahedral, decohedral and tetrahedral structure is established in this work. It is found N_t and λ have reverse contribution to B_a, that is B_a increases with N_t increasing, while decreases with λ increasing. As the basic parameter, size- and shape-dependent B_a function is extended to predict the cohesive energy $E_c(N_t)$ of quantum dots. Similar to B_a, $E_c(N_t)$ behaves as strong dependence on both size and shape. Larger N_t leads to higher $E_c(N_t)$, whereas larger λ results in smaller $E_c(N_t)$ value. There is a sequence: E_c(IH) > E_c(CO) > E_c(truc-DH) > E_c(OT) > E_c(DH) > E_c(TH) if N_t is certain, which is same to B_a since B_a(IH) > B_a(CO) > B_a(truc-DH) > B_a(OT) > B_a(DH) > B_a(TH) is tested in whole size range. To some extent, this is due to λ(IH) = λ(truc-DH) < λ(CO) < λ(OT) < λ(DH) < λ(TH), however, there is B_a(IH) > B_a(truc-DH) despite λ(IH) = λ(truc-DH). In addition, λ is

* Author to whom any correspondence should be addressed: E-mail:lihui02@tyut.edu.cn. liming2010@chnu.edu.cn.

no longer a constant and increases with N_t increasing when shape is given. The fact that whatever shape is, B_a or $E_c(N_t)$ increases with N_t increasing, means shape is the secondary factor if compared with size. The validity of the size- and shape-related model for $E_c(N_t)$ function is also confirmed by the simulation results of the size- and shape-dependent thermodynamic stability in Au, Ag, Cu, Ca, Sr, and Si quantum dots with different atomic structures.

Keywords: bond number, shape factor, size effect, cohesive energy, quantum dots

1. Introduction

Nanocrystalline quantum dots with large surface-to-volume ratio have been intensively studied due to their unique chemical and physical properties compared with those of their counterpart bulk crystals [1-4]. Some of the applications of these materials is to act as catalysts [5-10], nanodevices [11, 12], and life science [13, 14]. This tremendous increase in the interest in quantum dots is substantially motivated by rapid changes in materials properties as a function of the particle size and the relatively recently acquired abilities to synthesize such small particles of many materials with great control of size and shape [15]. However, geometry and symmetry vary as particle size decrease where evident size effects are observed partly due to the increase of the surface/volume ratio [16-18]. For example, the equilibrium structure of Au, Ag, Cu and Ni quantum dots predominantly consist of icosahedrons, tetrahedrons, and decahedrons, while their bulk structures are fcc (faced-center-cubic) structure [19, 20]. The sequential growth of Cu clusters demonstrates structural changes from triangle to icosahedron and finally to fcc with size increasing [21].

Since a limited number of atoms in quantum dots, the shape or morphology becomes an inevitable factor in determining their properties [22-25], except size effect. This is confirmed by the fact that stable phase depends on the shape of the quantum dot if size is certain [15], despite the majority of the experimental results being for spherical quantum dots. It also has been experimentally demonstrated that the change of the shape resulted in a considerable amount of depression in melting temperature [26], because the ratio of the atomic number at the surface to that in the volume is related

with shape. Thus, both size and shape effects should be concerned for quantum dots. To simultaneously reflect these two factors, bond number (B_a), which denotes the total atomic bond number in a system, is a good choice. Moreover, the size- and shape-related bond number could directly alter the cohesive energy $E_c(N_t)$ with N_t being the total atoms number. There is $E_c(N_t) = B_a \times \varepsilon$, if ε denotes the single bond energy in a system. Thus, if shape or size is changed, B_a could be altered and then modifies some of the basic material properties [3], including $E_c(N_t)$ and even melting.

Recently, Jiang et al. have proposed the following expression to determine the size-dependent cohesive energy [5]:

$$E_c(N_t)/E_{c0} = [B_a/B_t + (B_a/B_t)^{1/2}]/2 \quad (1)$$

where E_{c0} denotes the corresponding bulk cohesive energy, and B_t is the total bond number without any broken bond for the system with N_t atoms. From Eq. (1), as long as B_a/B_t is known, $E_c(N_t)$ function can be resolved, and then used to estimate other properties, such as surface energy, melting temperature, Curie transition temperature, Debye temperature, diffusion activation energy, and vacancy formation energy [3, 27, 28]. From geometric point, both B_a and B_t are the function of N_t and can be read:

$$B_a = [Z_s N_s + Z_b(N_t - N_s)]/2 \quad (2.1)$$

$$B_t = [Z_b N_t]/2 \quad (2.2)$$

where Z_s is the average coordination number of surface atoms, Z_b is the coordination number of bulk interior atoms, and N_s being the number of surface atoms. In terms of Eqs (1) and (2), B_a/B_t and $E_c(N_t)$ have great dependence on N_t with B_a/B_t (or $E_c(N_t)/E_{c0}$) $\rightarrow 1$ when $N_t \rightarrow \infty$. However, if N_t is given, B_a is not always a constant,

behaving as strong dependence on shape. For example, when N_t = 13, one get B_a = 42 for icosahedral structure, while B_a = 37 for truc-decohedral structure. However, both of them are the segment from face-centered-cubic and they have B_t (= 78). As a result, the shape effect should be concerned in analyzing B_a/B_t or $E_c(N_t)$ function. In some previous works [29, 30], shape factor λ is taken as the parameter to describe shape effect. Usually λ is defined as the surface area ratio between non-spherical and spherical quantum dots with identical N_t values, and moreover λ is taken as a constant for a given shape. For example, Lu et. al calculated λ = 0.66 if quantum dot adopts as icosahedral shape, while λ = 1.23 and λ = 2.45 respectively for octahedral and tetrahedral structure. However, a detailed study is lacking on the shape effect on B_a or $E_c(N_t)$, and moreover whether λ is a constant is not clear. This knowledge is important to understand the phenomena of the cohesion and to correlate the cohesive energy of different shapes.

In this work, the shape factor λ and its relation with size is considered and applied in resolving B_a and B_t for the quantum dots respectively with icosahedral (IH), truc-decohedral (truc-DH), cuboctahedral (CO), octahedral (OT), decahedral (DH), and tetrahedral (TH) atomic structure. And then, the size and shape influence on B_a/B_t and even on $E_c(N_t)/E_{c0}$ are analyzed by using this model. For any atomic structure or shape, λ behaves as strong size dependent and decreases with N_t dropping, which is in favor of the increase in B_a/B_t or $E_c(N_t)/E_{c0}$. However, B_a/B_t or $E_c(N_t)/E_{c0}$ still decreases with N_t dropping whatever shape is. If N_t is fixed, the sequences of B_a(CO) > B_a(truc-DH) > B_a(OT) > B_a(DH) > B_a(TH) and E_c(IH) > E_c(CO) > E_c(truc-DH) >

E_c(OH) > E_c(DH) > E_c(TH) are obtained, while λ(IH) = λ(truc-DH) < λ(CO) < λ(OT) < λ(DH) < λ(TH) is seen. To confirm the validity of the established model for size- and shape-related B_a/B_t, the simulation results for $E_c(N_t)$ of Au, Ag, Cu, Ca, Sr, and Si quantum dots are taken and compared with model predictions.

2. Model

To establish λ function, the spherical shape is introduced, and it has $\lambda \equiv 1$ in whole size range. However, for other nonspherical shape, the parameter λ is no longer a constant even shape is ensured. According to the definition for λ, which is the ratio of surface to volume (δ) in a nonspherical quantum dot to that (δ) in a spherical quantum dot with identical N_t value, λ can be written as:

$$\lambda = \delta/\delta \quad (3)$$

where $\delta = N_s/N_t$, and $\delta = D_0/D = 6h/D$ for a spherical quantum dot, where D_0 is the critical diameter with all atoms being on the surface, D is the diameter of a spherical quantum dot and h being atomic diameter. Eq. (3) can then be written as $\lambda = (N_s/N_t)/(6h/D)$. It is clear that λ is not only related with size, but also with shape, since both N_s and N_t of quantum dots are influenced by atomic structure or shape. For example, the smallest system has N_t =13 and N_s = 12 for IH structure, while N_t = 38 and N_s = 32 for CO structure and has $N_t = N_s = 4$ for TH one. Thus, λ is directly related with shape since δ is changed by shape even they have same N_t value.

To simplify the resolution of λ, it is necessary to unify the units of D and N_t. With the help of the lattice packing density η, which denotes the ratio of the volume of the crystal occupied by the atoms to the total volume, N_t can be determined as N_t =

$\eta V/V_a$, where V_a denotes the volume of an atom and is equal to $\pi h^3/6$ if the atom is regarded as ideal sphere. The V being the volume of quantum dots with spherical shapes can be obtained by using $V = \pi D^3/6$. Thus, there is $N_t = \eta D^3/h^3$, and then D can be written as:

$$D = h \times \sqrt[3]{N_t / \eta} \tag{4}$$

Then, the size- and shape-related λ has the following expression:

$$\lambda = \left[N_s / N_t\right] \Big/ 6 \times \sqrt[3]{\eta / N_t} \tag{5}$$

In Eq. (5), η value for particular standard crystal structure such as face-centered cubic, body-centered cubic, simple cubic, and hexagonal closed-paced structures can be found in the literature [31]. In this work, $\eta = 0.74$ is utilized [30], since the IH, truc-DH, CO, OT, DH, and TH structures are the segments of face-centered cubic crystal. It should be noted that Eq. (5) indicates that λ is meaningful only if the N_t value of a spherical structure is equal with those of other shapes. Clearly, the size and shape dependence of λ can be reflected by both N_s and N_t. Based on the geometric characteristics of quantum dots with different shape, N_s and N_t can be expressed:

$$N_s = 10(n-1)^2 + 2, \quad N_t = 10n^3/3 - 5n^2 + 11n/3 - 1 \quad \text{(IH)} \quad (6.1)$$

$$N_s = 10(n-1)^2 + 2, \quad N_t = 10n^3/3 - 5n^2 + 11n/3 - 1 \quad \text{(truc-DH)} \quad (6.2)$$

$$N_s = 30n^2 - 60n + 32, \quad N_t = 16n^3 - 33n^2 + 24n - 6 \quad \text{(CO)} \quad (6.3)$$

$$N_s = 4n^2 - 8n + 6, \quad N_t = 2n^3/3 + n/3 \quad \text{(OT)} \quad (6.4)$$

$$N_s = 5n^2 - 10n + 7, \quad N_t = 5n^3/6 + n/6 \quad \text{(DH)} \quad (6.5)$$

$$N_s = 2n^2 - 4n + 4, \quad N_t = n^3/6 + n^2/2 + n/3 \quad \text{(TH)} \quad (6.6)$$

where n (integer) is the atoms number on one edge. In this study, $n \geq 2$ is required,

since all of the structures possess only one atom if $n = 1$. From Eq. (6), N_s and N_t rely on both n and shape.

Fig. 1 displays the change of λ for different atomic structures with respect to size. For any nonspherical atomic structures, λ strongly depends on N_t and increases with N_t increasing. One can find when $n = 2$, λ(IH) = λ(truc-DH)≈ 0.33, λ(CO) ≈ 0.52, λ(OT) ≈ 0.33, λ(DH) ≈ 0.35, and λ(TH) ≈ 0.30; and when $n = 10$, λ(IH) ≈ 0.74, λ(CO) ≈ 0.81, λ(OT) ≈ 0.78, λ(DH) ≈ 0.85, and λ(TH) ≈ 0.83. This trend can also be expected for other structures. This means, λ is determined by N_t, which is different from the usual consideration for λ. In some literatures[17, 18], λ is usually taken as a constant if the shape is given. In addition, the difference among these curves implies that λ is shape related, except spherical quantum dots having $\lambda = 1$. From Fig. 1, if let N_t fixed, the λ values of the quantum dots follow this order: λ(IH) = λ(truc-DH) < λ(CO) < λ(OT) < λ(DH) < λ(TH). This sequence can be extended even in the entire size range. IH or truc-DH structure always has the smallest λ value, whereas TH structure possesses the largest one.

In fact, the size and shape effect on λ arises from δ which ranges from 0 to 1. As shown in Fig. 2, N_s increases as N_t increases ($\delta \to 0$), and $N_s \to N_t$ as $N_t \to 0$ ($\delta \to 1$). Note the variation of N_s with N_t relies strongly on shape, and there is N_s(IH) = N_s(truc-DH) < N_s(CO) < N_s(OT) < N_s(DH) < N_s(TH), if N_t is given. This is consistent with the sequence of λ. Thus, the strong dependence of λ on size and shape implies the bond number is also greatly changed by size and shape. To establish the size- and shape-related bond number, the ratio of B_a/B_t is taken. With the help of Eq. (2), B_a/B_t

has the following expression.

$$\frac{B_a}{B_t} = \frac{Z_s N_s + Z_b (N_t - N_s)}{Z_b N_t} \tag{7.1}$$

or,

$$\frac{B_a}{B_t} = \frac{Z_s \delta' + Z_b (1 - \delta')}{Z_b} \tag{7.2}$$

By introducing the parameter λ into Eq. (7), the size- and shape-dependent B_a/B_t will be written as:

$$\frac{B_a}{B_t} = \frac{6 Z_s \lambda / \sqrt[3]{N_t / \eta} + Z_b (1 - 6\lambda / \sqrt[3]{N_t / \eta})}{Z_b} \tag{8}$$

From Eq. (8), B_a/B_t is directly related with λ and N_t. Except this, Z_s should be concerned. According to the geometric characteristics, Z_s is read,

$$Z_s = \frac{45n^2 - 105n + 66}{5(n-1)^2 + 1} \quad \text{(IH)} \tag{9.1}$$

$$Z_s = \frac{85n^2 - 205n + 132}{10n^2 - 20n + 12} \quad \text{(truc-DH)} \tag{9.2}$$

$$Z_s = \frac{132n^2 - 294n + 168}{15n^2 - 30n + 16} \quad \text{(CO)} \tag{9.3}$$

$$Z_s = \frac{18n^2 - 48n + 36}{2n^2 - 4n + 3} \quad \text{(OT)} \tag{9.4}$$

$$Z_s = \frac{45n^2 - 115n + 82}{5n^2 - 10n + 7} \quad \text{(DH)} \tag{9.5}$$

$$Z_s = \frac{9n^2 - 27n + 24}{n^2 - 2n + 2} \quad \text{(TH)} \tag{9.6}$$

Z_s also has great dependence on size and shape. In Fig. 3, one can find that Z_s increases with N_t increasing for any shape. As $N_t \to \infty$, $Z_s \to 9$ for IH, OT, DH, TH structures, while $Z_s \to 8.5$ and $Z_s \to 8.8$ respectively for truc-DH and CO structures.

From Fig. 3, in the whole size range, one cannot find a certain sequence for Z_s values among these shapes. It seems IH structure has the largest Z_s value and truc-DH has the smallest value. Even this, the obvious size and shape dependence of Z_s still exists.

With the help of Eqs (1) and (8), the size- and shape-dependent cohesive energy for quantum dots with different shape can be written as,

$$E_c(N_t)/E_{c0} = \{ \frac{6Z_s\lambda/\sqrt[3]{N_t/\eta} + Z_b(1-6\lambda/\sqrt[3]{N_t/\eta})}{Z_b} + \left\{ \frac{6Z_s\lambda/\sqrt[3]{N_t/\eta} + Z_b(1-6\lambda/\sqrt[3]{N_t/\eta})}{Z_b} \right\}^{1/2} \}/2 \quad (10)$$

Eq. (10) can be used to estimate $E_c(N_t)$ of quantum dots with any shape as long as λ, Z_s and the corresponding N_t are known. The geometric parameters: N_t, λ and Z_s are all related with size and shape, and moreover λ and Z_s are the function of N_t. That is to say, if shape and N_t are ensured, the λ and Z_s can be obtained, and then B_a/B_t and $E_c(N_t)/E_{c0}$ analyzed.

3. Results and discussion

Based on Eq. (8), Fig. 4a presents the size- and shape-dependent bond number B_a of the quantum dots with IH, truc-DH, CO, OT, DH, and TH structures, where all of them have $B_t = 6N_t$. Whatever shape is, B_a increases with N_t increasing , having $B_a \rightarrow 0$ as $N_t \rightarrow 0$ and $B_a \rightarrow B_t$ when $N_t \rightarrow \infty$. However, B_a drops with λ increasing, which can be found from the curves of Fig. 4b, where $N_t = 100$ is taken. Thus, one can say N_t and λ have reverse contribution to B_a. As seen in Fig. 4b, the difference among different structure is clear, which arises from the different Z_s values used in Eq. (8). In fact, if N_t is given, Z_s and λ values are known, because both of them are the monotonic

function of N_t. Thus, three parameters of N_t, Z_s and λ in Eq. (8) can be combined into one. Then, B_a becomes the function of size, but the size-related shape effect is included. In Fig. 4c, the change of B_a with size is shown for different shape, and the difference is also clear, which is due to shape effect especially for IH and TH structures. For truc-DH, CO, OT, DH structures, the difference is relatively small. As seen in Fig. 4c, if N_t is fixed, there is a sequence: B_a(IH) > B_a(CO) > B_a(truc-DH) > B_a(OT) > B_a(DH) > B_a(TH), which is due to λ(IH) < λ(CO) < λ(OT) < λ(DH) < λ(TH) to some extent. This means the contribution of Z_s to this sequence is minor, if compared with λ. But there is an exception, that is B_a(IH) > B_a(truc-DH) but existing λ(IH) = λ(truc-DH), because of Z_s(IH) > Z_s(truc-DH). It should be noted, B_a still increases with N_t increasing if shape is given. In this process, the increase in λ is accompanied, which will lead to the depression in B_a with size increasing. However, the sequence of B_a(IH) > B_a(CO) > B_a(truc-DH) > B_a(OT) > B_a(DH) > B_a(TH) can be found even in whole size range. Thus, size is the major effect on B_a function, and shape is the second one. However, size and shape should be simultaneously considered in determining B_a values.

Based on Eqs. (1) and (10), the change rule of $E_c(N_t)$ with N_t is similar with that of B_a. As shown in Fig. 5, the size- and shape-dependent $E_c(N_t)$ function are obvious. Similar with B_a, $E_c(N_t)$ increases with N_t increasing, while decreases with λ increasing. Moreover, same sequence of the thermodynamic stability with that of B_a are found if N_t is given, that is E_c(IH) > E_c(CO) > E_c(truc-DH) > E_c(OT) > E_c(DH) > E_c(TH). This sequence can be expected in whole size range, and also consist with the simulation

results. Thus, one can say, except size effect on $E_c(N_t)$, the decreased λ could enhance the thermodynamic stability with size decreasing by Eq. (10).

To confirm the validity of Eq. (10), the comparison of model predictions with the simulation results is made. The simulation results[5,32,33] shown in Figs 6-8 are all the results by first-principle calculation, since this techniques have proven to be a very good compromise between accuracy and computational efficiency. For example, Liu et al[5]. calculated the cohesive energy of Ag dots by DMOL code, in which each electronic wave function was expanded in a localized atom-centered basis set. and GGA-RPBE was employed as the exchange correlation function for Cu quantum dots[33]. In addition, Häberlen et al.[32] present the energetic characteristics of Au quantum dots with different shape by means of a scalar relativistic all-electron density functional method. In these figures, one can find, within the error range, the model predictions are in good agreement with the simulation results for icosahedral Ag [5], Au [32], and Cu [33] quantum dots, even if N_t is smaller than 200 as shown in Fig. 6. Moreover, the consistence with model predictions is seen for cobuoctahedral Ag [5], Au [32] and octahedral Au [32] quantum dots, respectively in Figs 7 and 8. In addition, the simulation results of Ca and Sr quantum dots respectively with IH, truc-DH, and CO shape further confirm the reasonability of Eq. (10), where the energetic characteristics of Ca and Sr quantum dots are obtained by using many-body atomistic potential of the Murrel-Mottram type[39]. All this displays $E_c(N_t)$ increases with N_t increasing, while decreases with λ increasing, which means both size and shape have great influence on $E_c(N_t)$.

Due to the lack of the simulation results for $E_c(N_t)$ of TH structure, we taken the Molecular Dynamics (MD) or the experimental results for the melting point $T_m(D)$ of tetrahedral Ag [34, 35], and Si [36, 37] nanoparticles for comparison. Since the approximate relationship between $T_m(D)$ and $E_c(D)$, where D is the diameter and has same means with N_t, there is $T_m(D) \propto E_c(D)$ [38]. As shown in Fig. 10, the solid lines are the prediction results for TH structure in terms of Eq. (10), and the symbols are the simulational and experimental results for the size-related $T_m(D)$ values. In the MD calculation results, the authors[35] used the embedded atom potential model to simulate the dynamics of tetrahedral Ag particles and obtain their melting point, and moreover the authors have successfully synthesized tetrahedral Ag particles by using the inert gas condensation technique to support their MD calculation. In experiments, Au nanoparticles are reported to be grown in an inert-gas beam and deposited on the end of a tungsten field emitter[34]. A size-dependent melting behavior of supported Au nanoparticle is obtained through observing the shape change by field-emission current method[34]. In the Refs [36,37], the melting temperature of supported Si nanoparticles was measurement by using a JEOL 100 electron microscope equipped with a low-drift heating stage, or using Raman scattering spectroscopy to obtain the crystallization temperature dependency on Si nanoparticles. Note that although the shapes of Si and Ag clusters are not mentioned definitely in the corresponding experiments[34,36,37], the trend and comparison results shown in Fig. 10 suggest that Si and Ag clusters may take the shape of tetrahedron. In Fig. 10, the results for Ag and Si TH nanoparticles are not so consistent with MD or experimental values. This difference maybe due to

the approximate relationship between $T_m(D)$ and $E_c(D)$. In addition, this difference implies the instability of TH structure. Although the existed errors, their change trends of $T_m(D)$ with size are still in consistence.

Given that the bond number is the basic parameter of quantum dots, and its deduction: cohesive energy is essential in describing the variations of thermodynamic and other parameters of quantum dots, the establishment of our model is important in quantitatively studying several basic problems of materials with regard to size and shape effects. By introducing shape factor and size effect into bond number, we can improve our model to predict more accurately and then several useful relations for nonspherical quantum dots can be in valid derived. The main advantage of our model is that there is no need to know surface energies and other thermodynamic information, and only atom number and shape are needed for calculating cohesive energy.

4. Conclusions

We proposed the size dependence of shape factor λ to account for the size- and shape-dependent bond number B_a of quantum dots with different shapes. Based on the λ function, the difference between the spherical and nonspherical nanoparticles was determined and their thermodynamic stability was compared. As expected, both size and shape have great influence on B_a, behaving as B_a decreases with N_t decreasing, while decreases with λ increasing if the size is given. It is also found $B_a(\mathrm{IH}) > B_a(\mathrm{CO}) > B_a(\text{truc-DH}) > B_a(\mathrm{OT}) > B_a(\mathrm{DH}) > B_a(\mathrm{TH})$ in the entire size range. This sequence can be extended to predict the thermodynamic stability of quantum dots,

resulting in E_c(IH) > E_c(CO) > E_c(truc-DH) > E_c(OT) > E_c(DH) > E_c(TH). Therefore, by knowing the nature and trend of cohesive energy change, it is possible to tune the cohesive energy of a solid by simply controlling the shape and size of the constituent solids.

Acknowledgement

The authors acknowledge the financial supports of the National Natural Science Foundation of China (grant No. 11404235 and No. 51301073), Natural Science Foundation of Shanxi Province (No. 2014011010 and No. 2015021107) and also supported by Program for the Top Young Academic Leaders of Higher Learning Institutions of Shanxi.

Captions:

Fig. 1.The shape and size dependence of λ by Eq. (5).

Fig. 2. The change trend of N_s with N_t in terms of Eq. (6) for IH, truc-DH, CO, OT, DH, and TH shapes, and the dashed lines indicates $N_s = N_t$.

Fig. 3. The size-related Z_s for IH, truc-DH, CO, OT, DH, and TH shapes by Eq. (9).

Fig. 4. (a) The size- and shape-related B_a/B_t functions, where red line denotes the IH structure, olive line is CO structure, magenta line is truc-DH one, blue line is OT one, dark yellow line is DH one and black line is TH one; (b) the change trend of B_a/B_t with λ when $N_t = 100$ is given; (c) the size-dependence of B_a/B_t quantum dots for IH, truc-DH, CO, OT, DH, and TH shapes.

Fig. 5. The size- and shape-related $E_c(N_t)$ function for IH (red line), truc-DH (magenta line), CO (olive line), OT (blue line), DH (dark yellow line), and TH (black line) shapes.

Fig. 6. The comparison of model prediction of Eq. (10) with the simulation results for $E_c(N_t)$ of Ag, Au, Cu icosahedral quantum dots which denoted as the symbols ■ [5], ▼[32], ▲[32] and ● [33].

Fig. 7. $E_c(N_t)$ function by Eq. (10) for Ag and Au quantum dots with CO shape. The corresponding simulation results are shown as the symbols ◆ [5], ►[32], ●[32], ▼[32], and ▲[32].

Fig. 8 The model predictions of Eq. (10) for Au quantum dots with OT shape, and the symbols ▲ and ▼ [32] are the corresponding simulation results.

Fig. 9. Comparisons of $E_c(N_t)$ function for Ca and Sr quantum dots respectively with

IH, truc-DH and CO shapes described by Eq. (10) with the available simulation results [39] with symbols showing experimental data as ■, ▲, ●, □, Δ and ○.

Fig. 10. The solid lines are the model predictions of $T_m(D)$ function for tetrahedral Ag and Si quantum dots with the help of Eq. (10). And the symbols ■ [34], ● [35], ▲ [36] and Δ [37] are the corresponding experimental results.

Fig. 1

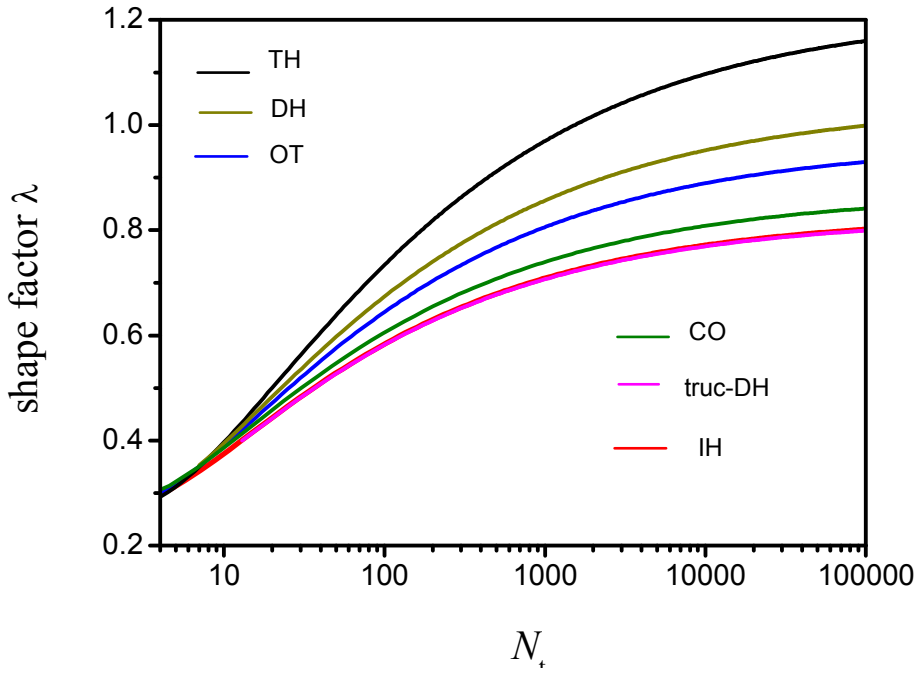

Fig. 2

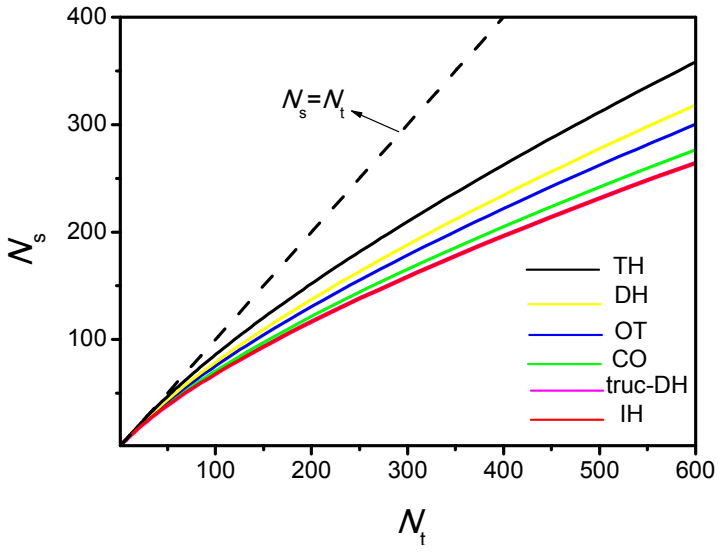

Fig. 3

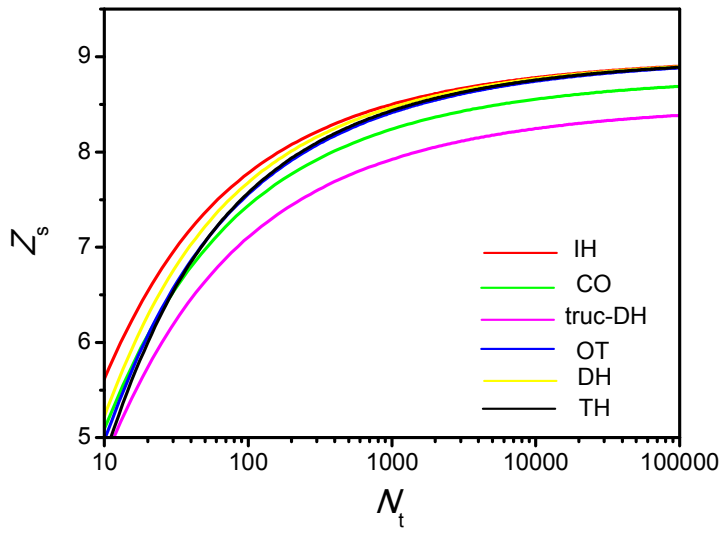

Fig. 4a

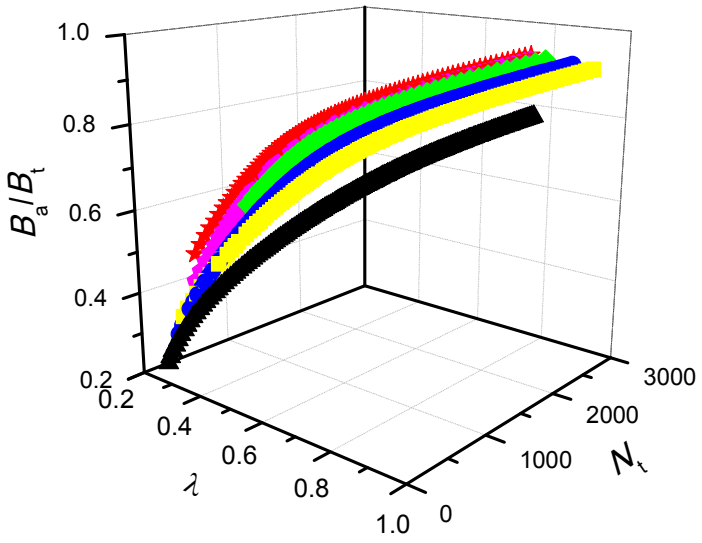

Fig. 4b

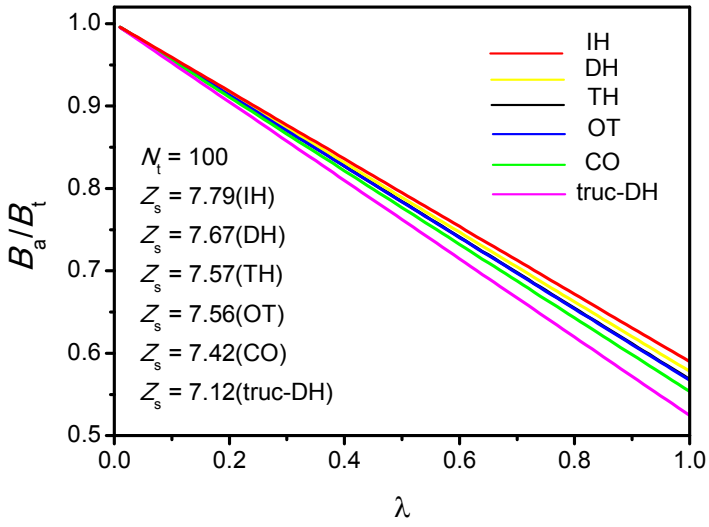

Fig. 4c

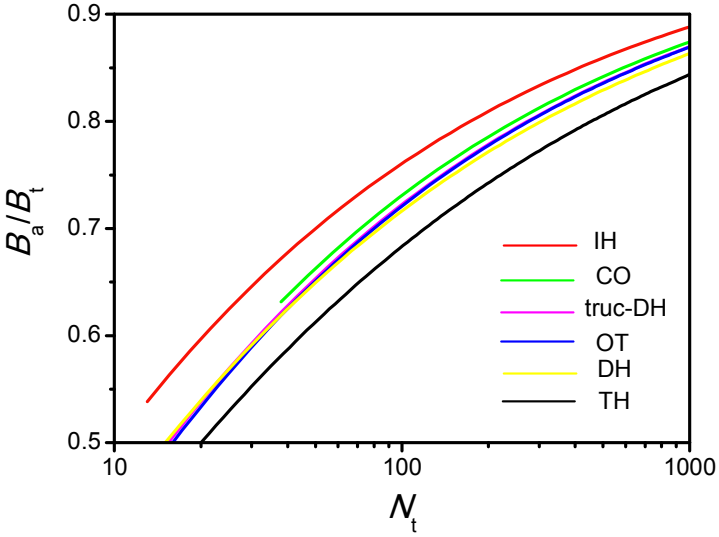

Fig. 5

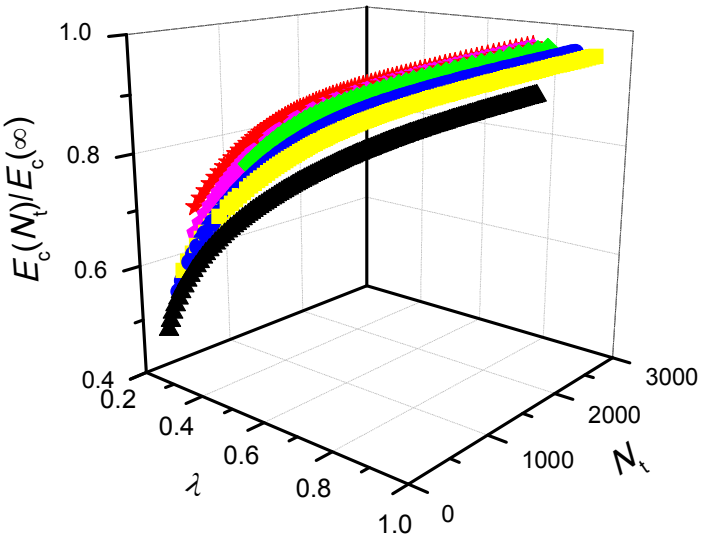

Fig. 6

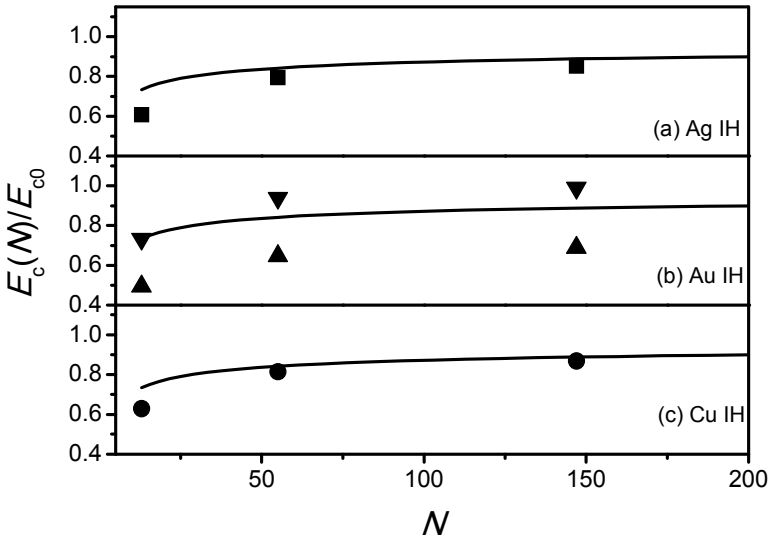

Fig. 7

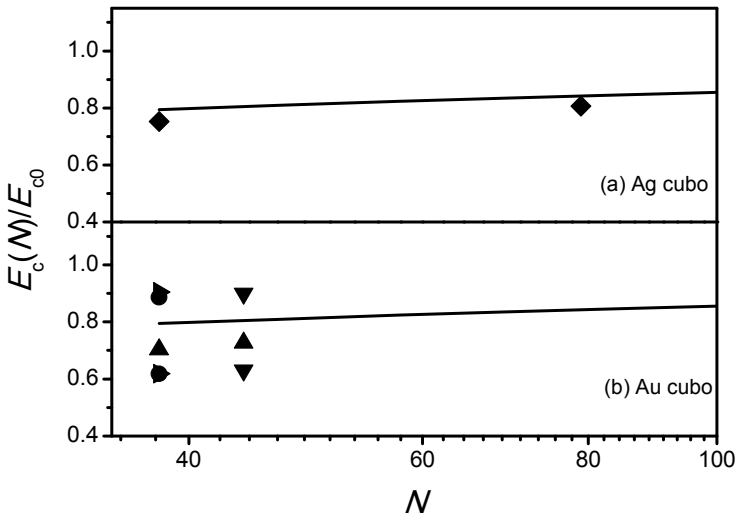

Fig. 8

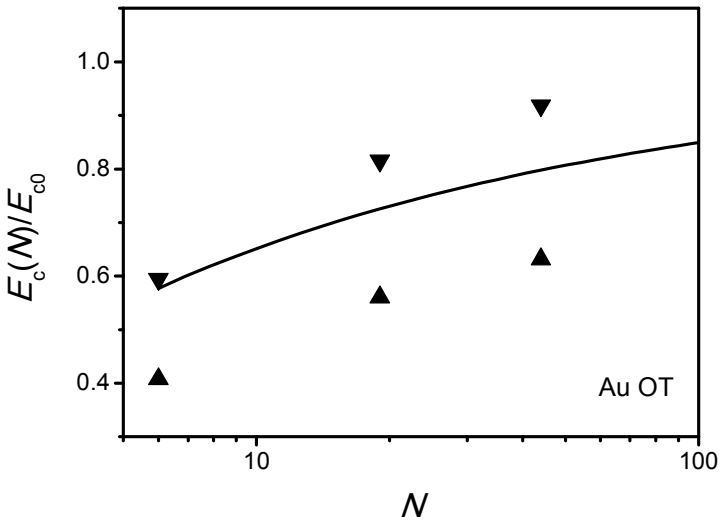

Fig. 9

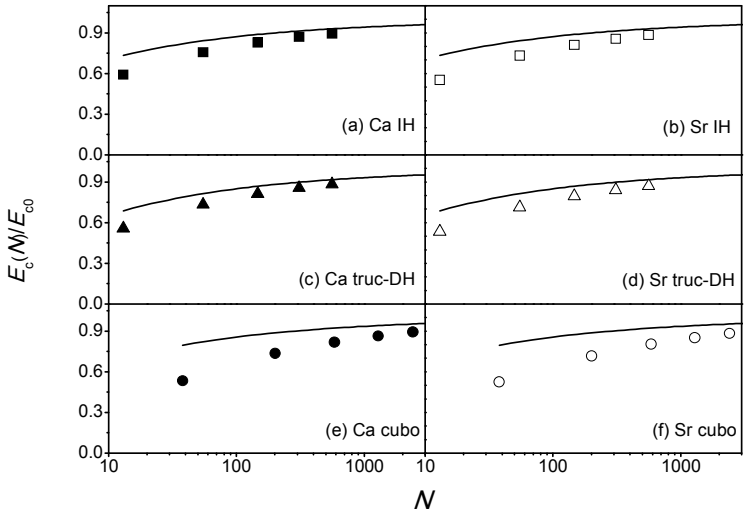

Fig. 10

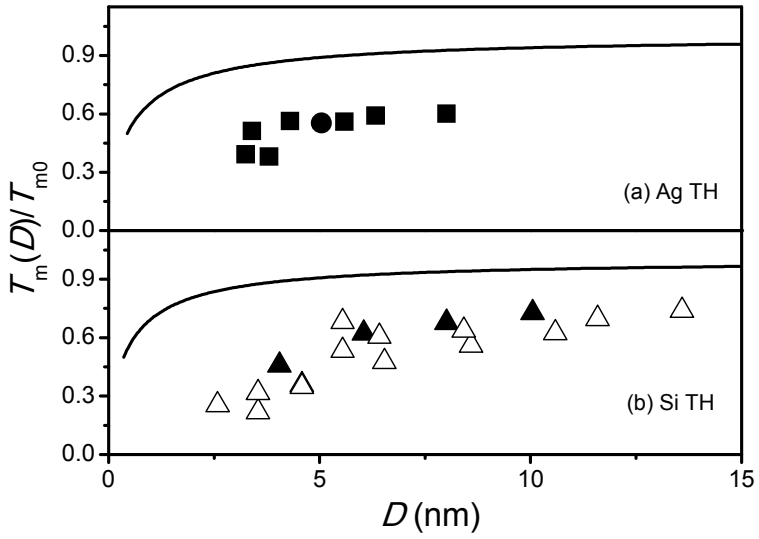

References

1. S. Laurent, D. Forge, M. Port, A. Roch, C. Robic, L. Vander Elst and R. N. Muller, *Chemical Reviews*, 2008, 108, 2064-2110.

2. T. K. Sau and A. L. Rogach, *Advanced Materials*, 2010, 22, 1781-1804.

3. C. C. Yang and Y.-W. Mai, *Materials Science and Engineering: R: Reports*, 2014, 79, 1-40.

4. Y. F. Zhu, J. S. Lian and Q. Jiang, *The Journal of Physical Chemistry C*, 2009, 113, 16896-16900.

5. D. Liu, J. S. Lian and Q. Jiang, *The Journal of Physical Chemistry C*, 2009, 113, 1168-1170.

6. C. Lemire, R. Meyer, S. Shaikhutdinov and H.-J. Freund, *Angewandte Chemie International Edition*, 2004, 43, 118-121.

7. Z.-P. Liu, P. Hu and A. Alavi, *Journal of the American Chemical Society*, 2002, 124, 14770-14779.

8. X. Zhou, W. Xu, G. Liu, D. Panda and P. Chen, *Journal of the American Chemical Society*, 2009, 132, 138-146.

9. D. Matthey, J. G. Wang, S. Wendt, J. Matthiesen, R. Schaub, E. Lægsgaard, B. Hammer and F. Besenbacher, *Science*, 2007, 315, 1692-1696.

10. O. Lopez-Acevedo, K. A. Kacprzak, J. Akola and H. Häkkinen, *Nature Chemistry*, 2010, 2, 329-334.

11. M. E. Stewart, C. R. Anderton, L. B. Thompson, J. Maria, S. K. Gray, J. A. Rogers and R. G. Nuzzo, *Chemical Reviews*, 2008, 108, 494-521.

12. J. N. Anker, W. P. Hall, O. Lyandres, N. C. Shah, J. Zhao and R. P. Van Duyne, *Nature Materials*, 2008, 7, 442-453.

13. M.-C. Daniel and D. Astruc, *Chemical Reviews*, 2004, 104, 293-346.

14. A. Sassolas, B. D. Leca-Bouvier and L. J. Blum, *Chemical Reviews*, 2007, 108, 109-139.

15. S. Datta, M. Kabir, T. Saha-Dasgupta and D. D. Sarma, *The Journal of Physical Chemistry C*, 2008, 112, 8206-8214.

16. K. Bao, S. Goedecker, K. Koga, F. Lançon and A. Neelov, *Physical Review B*, 2009, 79, 041405.

17. P. Gruene, D. M. Rayner, B. Redlich, A. F. G. van der Meer, J. T. Lyon, G. Meijer and A. Fielicke, *Science*, 2008, 321, 674-676.

18. Y. Gao, N. Shao, S. Bulusu and X. C. Zeng, *The Journal of Physical Chemistry C*, 2008, 112, 8234-8238.

19. D. Alamanova, V. G. Grigoryan and M. Springborg, *The Journal of Physical Chemistry C*, 2007, 111, 12577-12587.

20. V. G. Grigoryan, D. Alamanova and M. Springborg, *Physical Review B*, 2006, 73, 115415.

21. G. H. Guvelioglu, P. Ma, X. He, R. C. Forrey and H. Cheng, *Physical Review B*, 2006, 73, 155436.

22. S. Aksu, A. A. Yanik, R. Adato, A. Artar, M. Huang and H. Altug, *Nano Letters*, 2010, 10, 2511-2518.

23. N. Berkovitch, P. Ginzburg and M. Orenstein, *Nano Letters*, 2010, 10,

1405-1408.

24. G. A. Wurtz, PollardR, HendrenW, G. P. Wiederrecht, D. J. Gosztola, V. A. Podolskiy and A. V. Zayats, *Nature Nanotechnology*, 2011, 6, 107-111.

25. L. Sapienza, H. Thyrrestrup, S. Stobbe, P. D. Garcia, S. Smolka and P. Lodahl, *Science*, 2010, 327, 1352-1355.

26. R. Goswami and K. Chattopadhyay, *Philosophical Magazine Letters*, 1993, 68, 215-223.

27. C. C. Yang and Q. Jiang, *Acta Materialia*, 2005, 53, 3305-3311.

28. C. C. Yang and S. Li, *Physical Review B*, 2007, 75, 165413.

29. H. M. Lu, P. Y. Li, Z. H. Cao and X. K. Meng, *The Journal of Physical Chemistry C*, 2009, 113, 7598-7602.

30. W. H. Qi, M. P. Wang and Q. H. Liu, *Journal of Materials Science*, 2005, 40, 2737-2739.

31. H. M. Lu and Q. Jiang, *Physica Status Solidi (b)*, 2004, 241, 2472-2476.

32. O. D. Häberlen, S.-C. Chung, M. Stener and N. Rösch, *The Journal of Chemical Physics*, 1997, 106, 5189-5201.

33. W. Liu, D. Liu, W. T. Zheng and Q. Jiang, *The Journal of Physical Chemistry C*, 2008, 112, 18840-18845.

34. T. Castro, R. Reifenberger, E. Choi and R. P. Andres, *Physical Review B*, 1990, 42, 8548-8556.

35. M. Á. Gracia-Pinilla, E. Pérez-Tijerina, J. A. García, C. Fernández-Navarro, A. Tlahuice-Flores, S. Mejía-Rosales, J. M. Montejano-Carrizales and M. José-Yacamán,

The Journal of Physical Chemistry C, 2008, 112, 13492-13498.

36. M. Hirasawa, T. Orii and T. Seto, *Applied Physics Letters*, 2006, 88, 093119.

37. A. N. Goldstein, *Applied Physics A*, 1996, 62, 33-37.

38. C. Q. Sun, *Progress in Materials Science*, 2009, 54, 179-307.

39. J. E. Hearn and R. L. Johnston, *The Journal of Chemical Physics*, 1997, 107, 4674-4687.